

©2016, Elsevier. Licensed under the Creative Commons Attribution-NonCommercial-NoDerivatives 4.0 International <http://creativecommons.org/about/downloads>



# **Carbon-Cryogel Hierarchical Composites as Effective and Scalable Filters for Removal of Trace Organic Pollutants from Water**

Rosa Busquets<sup>1,3,7\*</sup>; Alexander. E. Ivanov<sup>2</sup>; Lubinda Mbundi<sup>1,5</sup>, Sofia Hörberg<sup>2</sup>, Oleksandr P. Kozynchenko<sup>3</sup>; Peter J. Cragg<sup>1</sup>; Irina N. Savina<sup>1</sup>; Raymond L.D. Whitby<sup>1,4</sup>; Sergey V. Mikhalovsky<sup>1,4</sup>; Stephen R. Tennison<sup>3</sup>; Hans Jungvid<sup>2</sup>; Andrew B.Cundy<sup>1,6\*</sup>.

<sup>1</sup>University of Brighton, Faculty of Science and Engineering, BN2 4GJ, UK

<sup>2</sup>Protista Biotechnology AB, Kvarngatan 2, P.O. Box 86 SE- 267 22 Bjuv, Sweden

<sup>3</sup>MAST Carbon International Ltd. Jays Close, Basingstoke, Hampshire RG22 4BA, UK†

<sup>4</sup>Nazarbayev University, School of Engineering, 53, Kabanbay Batyr Ave., Astana, 010000, Kazakhstan

<sup>5</sup>Blond McIndoe Research Foundation, East Grinstead, RH19 3DZ, UK

<sup>6</sup>University of Southampton, School of Ocean and Earth Science, Southampton, SO14 3ZH, UK.

<sup>7</sup>Kingston University, Faculty of Science, Engineering and Computing, Kingston Upon Thames, KT1 2EE, UK

Keywords: composite materials, hierarchical structures, phenolic carbon, cryogel, water treatment

## **Author information**

\* e-mail: [A.Cundy@soton.ac.uk](mailto:A.Cundy@soton.ac.uk)

\* e-mail: [R.Busquets@Kingston.ac.uk](mailto:R.Busquets@Kingston.ac.uk),

## Abstract

Effective technologies are required to remove organic micropollutants from large fluid volumes to overcome present and future challenges in water and effluent treatment. A novel hierarchical composite filter material for rapid and effective removal of polar organic contaminants from water was developed. The composite is fabricated from phenolic resin-derived carbon microbeads with controllable porous structure and specific surface area embedded in a monolithic, flow permeable, poly(vinyl alcohol) cryogel. The bead-embedded monolithic composite filter retains the bulk of the high adsorptive capacity of the carbon microbeads while improving pore diffusion rates of organic pollutants. Water spiked with organic contaminants, both at environmentally relevant concentrations and at high levels of contamination, was used to determine the purification limits of the filter. Flow through tests using water spiked with the pesticides atrazine (32 mg/L) and malathion (16 mg/L) indicated maximum adsorptive capacities of 641 and 591 mg pollutant/g carbon, respectively. Over 400 bed volumes of water contaminated with 32 mg atrazine/ L, and over 27400 bed volumes of water contaminated with 2 µg atrazine/ L, were treated before pesticide guideline values of 0.1 µg/L were exceeded. High adsorptive capacity was maintained when using water with high total organic carbon (TOC) levels and high salinity. The toxicity of water filtrates was tested *in vitro* with human epithelial cells with no evidence of cytotoxicity after initial washing.

## HIGHLIGHTS

- A novel hierarchical composite filtration material was developed for water treatment.
- The material contains porous phenolic carbon beads embedded in polyvinyl alcohol cryogel.

- Adsorptive capacities were 641 mg atrazine and 591 mg malathion per gram of carbon.
- High adsorption was maintained in water with high organic carbon levels and salinity.
- There was no evidence of toxicity to human epithelial cells after initial washing.

## **1. Introduction**

A wide range of contaminants are continuously released into waterways as a result of anthropogenic activity, many of which are not effectively removed by current waste water treatment processes (Wilkinson et al., 2016; Loos et al., 2013). Problem contaminants commonly comprise agrochemicals, pharmaceuticals, hormones, plasticisers, flame retardants, personal care products and food additives (Homem et al., 2015; Kokotou et al., 2012; Richardson and Ternes, 2014). These organic compounds are distributed across different environmental systems (e.g. soils, sediments, surface and ground waters), and the most polar (e.g. amines, alcohols or carboxylic acids and derivatives with small hydrocarbon skeletons and low partition coefficients) are bioavailable and may persist in the aqueous phase. These contaminants are now ubiquitous, and even at very low environmental concentrations (e.g. below 0.5 µg/L in surface and ground water, Cabezam et al., 2012; Loos et al., 2013; Sorensen et al., 2015) can potentially cause ecological changes and contaminate water supplies with (in some cases) unknown consequences for human health (Fent et al., 2006; Jeong et al., 2012). There is therefore a pressing need to purify water to safe (i.e. sub-ppb or ppt) levels. A range of technologies have been proposed to remove trace organic contaminants from waste and other waters, including chemical oxidation and improved adsorption methods, often using activated carbons. Indeed, in advanced waste water treatment processes, Granulated Activated Carbon (GAC) is used as a relatively low cost bulk

adsorbent and is recognised as an industry standard. However, the adsorptive capacity of GAC diminishes over time, and it shows relatively poor adsorptive uptake for a range of more polar organic contaminants such as estrogens, pharmaceuticals and some pesticides (Busquets et al., 2014; Cabezam et al., 2012; Ifelebuegu et al., 2011). This has led to a number of studies examining the potential of “designer” activated carbons, where control over the pore architecture is attempted to target particular dissolved species, to improve polar contaminant removal (Busquets et al., 2014; Gueudré et al., 2014; Ji et al., 2010; Unur, 2013; Zhang et al., 2011). In addition, use of hierarchical porous materials has been suggested to enhance mass transfer properties (Gueudré et al., 2014) and provide more effective adsorption of trace contaminants from water.

The present work explores the design of a flexible and scalable hierarchical composite filter comprised of phenolic resin-derived carbon microbeads with optimised micro-, meso- and macroporous structure embedded in a monolithic, flow permeable poly(vinyl alcohol) cryogel for the removal of small size, polar pesticides. Atrazine, (a herbicide of the triazine class, 2-chloro-4-ethylamino-6-isopropylamino-1,3,5-triazine,  $\log K_{ow}$  2.75; US EPA, 2006), and malathion, (an organophosphate insecticide, diethyl[(dimethoxyphosphinothioyl)thio]butanedioate,  $\log K_{ow}$  2.36–2.89; WHO, 2004), which enter waterways via runoff from agricultural land and have been frequently detected in surface or ground water (Fadaei et al., 2012; Nogueira et al., 2012; Sorensen et al., 2015; Varca, 2012), are used as model compounds to assess and optimise the water filters. Application and scalability are also discussed.

## 2. Materials and methods

**Materials.** The sources and purities of the chemicals used are provided in the Supporting Information S1. GAC was kindly provided by a UK water company.

**Synthesis of carbon microbeads.** Spherical activated carbon microbeads were obtained from Novolac phenol-formaldehyde resin with an average molecular weight 700-800 D (Hexion Specialty Chemicals Ltd., UK) following the technology patented by Tennison *et al.* (Tennison *et al.*, 2000). Briefly, micro-, meso- and macroporous phenolic resin-derived carbon beads were prepared by pyrolysis and physical activation in carbon dioxide. Beads were tailored by dissolving Novolac resin (100 weight parts) and cross-linking agent hexamethylenetetramine (20 weight parts) in varying quantities of ethylene glycol (180 – 300 weight parts for micro-, meso- (TE3), and macroporous (TE7) resins respectively). The resin suspension was then heat-cured in mineral oil. After removing the ethylene glycol (which acts as a solvent and pore former) by hot water washing or vacuum drying, the resin beads were ready for processing into carbons. The amount of carbon loss (burn-off) during activation with CO<sub>2</sub> was 34% and 55% in carbon beads denoted in this work as TE3 and TE7, respectively and the particle size studied ranged from 40 to 250µm. The structural features of the carbon beads are summarised in Supporting information S2.

**Preparation of polymer scaffold and composite filter.** Monolithic macroporous polymer “scaffolds” (Macroporous Polymer Structures (MPPS<sup>TM</sup>)) produced by the authors (Protista), also referred to as cryogels, were prepared by chemical cross-linking of polyvinyl alcohol (PVA) at -12 °C and used to support the carbon beads. PVA was dissolved at a concentration of 5% w/v in boiling water and cooled to room temperature. Hydrochloric acid (1M, 0.8 mL) was mixed with the PVA solution (7.2 mL) and kept in an ice bath for 30 min. Glutaraldehyde solution (75 µL, glutaraldehyde: water 50:50 v/v) and carbon beads (40-60µm diameter, 320 mg) were added to the cooled PVA solution with stirring. The mixture was poured into Ø3 × 100 mm glass tubes. The sealed tubes were placed into a cryostat (Arctest, Finland) at – 12 °C overnight. The cryogels were rinsed with water, then placed in sodium cyanoborohydride solution (0.1M, pH 9.2) overnight to reduce the residual aldehyde

groups, and finally rinsed with 4 bed volumes of water. The cryogels containing carbon beads were  $\varnothing 3 \times 85$  mm (0.6 mL) in size when non-hydrated and were used in this configuration for flow through studies.

**Structural characterisation.** The structure of the prototypes and GAC was analysed using low temperature nitrogen adsorption-desorption isotherms and scanning electron microscopy (Supporting Information S2, 3). The mechanical properties of the composites were tested with a T.A. *XTPplus* texture analyser equipped with a 1cm diameter cylindrical probe (Stable Micro Systems, UK). The composite samples were compressed with steadily increasing force of 5 N/min from 0.01N to 20N at room temperature. The stiffness was assessed as the stress necessary to achieve 75% compression. The Young's modulus of elasticity  $E$ , which is the slope of the stress-strain curve in the range of linear proportionality of stress to strain, has been calculated using equation (1), where  $F$  is the applied force;  $A$ , the cross-sectional area;  $L$ , the unstressed height; and  $\Delta L$ , the change in height due to  $F$ ;  $F/A$  (in compression or tension) is the stress and  $\Delta L/L$  is the strain.

$$E = (F/A) / (\Delta L/L) \quad (1)$$

The stress-strain curve obtained for the composite carried out immediately after a filtration test is shown in Supporting Information S4.

**Adsorption experiments.** Adsorption tests were carried out in batch mode under equilibrium conditions using an orbital shaker at 90 rpm, 25 °C for 48h or magnetic stirring. To assess breakthrough curves in the high capacity carbon-cryogel prototypes using realistic volumes of water at laboratory scale, it was necessary to filter highly contaminated water. Hence, pesticides concentrations were high (32 mg atrazine and 16 mg malathion per L) relative to environmental concentrations. Ethanol (1.4%) was added to stabilise the contaminants in aqueous solution and prevent their precipitation, which would cause overestimation of the

removal capacity of the developed prototypes. Batch adsorption tests were also carried out at more environmentally relevant contamination levels of 2 µg atrazine/L. For determination of the diffusion coefficient of atrazine and kinetics of its uptake, carbon beads (15 mg), or carbon-cryogel composites cut into cubes of 2 mm sides containing an equivalent mass of carbon beads (15mg), were incubated with spiked water (40 mL). Details on the quantification of adsorption capacity and pore diffusion kinetics are given in Supporting Information S3.

**Flow through adsorption studies.** Contaminated water was filtered continuously through the carbon-cryogel composite or a column packed with only carbon beads until saturation, using a peristaltic pump equipped with silicone tubing. Fractions of the filtrate were collected for analysis. Selectivity for removal of atrazine (32 mg/L) and malathion (16 mg/L) was studied with: (a) ultrapure water containing ethanol (1.4%); (b) a “model” water with high total carbon prepared by dissolving potassium hydrogen phthalate in aqueous solution (to mimic high-COD water) and ethanol (1.4%); and (c) water from the Ouse estuary (collected from Newhaven harbour, East Sussex, UK). The composition of the estuarine water (c) before spiking (and before adding 1.4% ethanol) was 19.2 mg/L total carbon; 12.7 mg/L inorganic carbon; 6.5 mg/L total organic carbon (TOC); Na<sup>+</sup> 9320 mg/L; K<sup>+</sup> 514 mg/L, Mg<sup>2+</sup> 1261 mg/L and Ca<sup>2+</sup> 339 mg/L as major ions. The pH was 8.1. The methodology used for the water analysis is given in the Supporting information S5. To assess adsorption at low (more environmentally relevant) concentrations, breakthrough curves were also determined using 2 µg atrazine/ L spiked ultrapure water.

**Analysis of atrazine and malathion.** Atrazine and malathion were quantified using d<sub>5</sub>-atrazine (atrazine with fully deuterated N-ethyl moiety) as an internal standard. Quantification was by LC-MS. Chromatographic and MS operating conditions are provided in the Supporting Information S5.



**Modelling.** The dimensions of atrazine and the minimum pore volume in a 3D carbonaceous structure for its adsorption were modelled using the Build interface in Spartan '10 software. Geometry optimisation was achieved using the semi-empirical quantum chemistry method PM6 from an initial structure calculated using molecular mechanics (Merck Molecular Force Field - MMFF).

**Cytotoxicity study.** The toxicity of ultrapure water filtered through the carbon-cryogel composites was tested on heterogeneous human epithelial colorectal adenocarcinoma cells (Caco-2). Cell viability was assessed *in vitro* using the lactate dehydrogenase (LDH) (Smith et al., 2011) and MTS assays (Malich et al., 1997). The cell culture methods and materials used are described in Supporting Information S6.

Data analysis

Statistical treatment: a t-student significance test, with P 0.05, was used to assess the adsorption of atrazine by PVA scaffolds without carbon beads; compare the content of carbon surface functional groups in the different carbons synthesized; and compare the viability of cells when treated with fractions of water filtrate

### **3. Results and discussion**

#### **Synthesis and application of phenolic carbon beads for water treatment.**

A graphite-like lattice of activated carbon contains a cloud of delocalised electron density that favours the adsorption of organic compounds, especially if they are aromatic, via  $\pi$ - $\pi$  interaction. Pores of appropriate size can add additional interaction between the pollutant and the carbon, and can significantly enhance removal, which is particularly poor for polar and small organic molecules. With atrazine as an example of a ubiquitous micropollutant in surface water, we have modelled and synthesised porous carbon sorbents for its optimal

removal from water. The dimensions of the optimal pores in the carbonaceous material that would present the highest interaction with atrazine and produce a state of minimal energy were derived using molecular mechanics (MMFF force field) and semi-empirical (PM6) methods and are shown in **Figure 1**. Large micropores (1.0-1.7 nm width) and mesopores (2-50 nm) in the low size range are predicted to be the preferential sites for the adsorption of the study contaminant.

For standard GAC used in the waste water industry, the maximum adsorptive capacity for atrazine was  $52.2 \pm 6.8$  mg/g (20 mg of GAC was incubated with 40 ml of 32 mg/L atrazine containing 1.4% ethanol in water, in batch conditions until equilibrium). The surface area of GAC determined from the nitrogen adsorption-desorption isotherm was  $552 \text{ m}^2/\text{g}$ . Given the dimensions of atrazine estimated in **Figure 1**, approximately 18% of the surface area of GAC was covered with the herbicide at equilibrium conditions.

The nitrogen adsorption-desorption isotherm also revealed that the GAC was mainly a microporous sorbent, with pores of 1.1-2.0 nm width, and hence appropriate for the removal of the herbicide according to the model shown in **Figure 1**. This model assumed that a size-exclusion effect found for bulky compounds (Ji et al., 2010) would not occur. However solvation could increase the effective solute dimensions and hinder access to micropores.

Aside from well-developed microporosity, the GAC has very low mesoporosity, in the range of 2.1-3.8 nm, and macropores were not detected. The absence of (meso- and macroporous) transport pores hinders the accessibility of the micropores, which can explain in part the low adsorptive capacity observed under high concentrations of atrazine.

To maximise pesticide removal, porous carbon microbeads with larger surface area and higher meso- and macropore volume compared to GAC were prepared. The porosity was primarily controlled by the amount of the pore former, ethylene glycol, which is entrapped in the liquid form within the phenolic resin when it solidifies in contact with hot mineral oil.

Washing out the entrapped ethylene glycol creates the porous structure in the polymeric precursor of activated carbon. In contrast, in the absence of the pore former, the oligomer chains cross-link, increase in weight and precipitate. Secondly, the activation stage, which was carried out at 900 °C in a CO<sub>2</sub> atmosphere, caused an increase of the number of micropores and the specific surface area and a slight widening of the meso- and macropores, depending on the activation degree, starting from 30% burn-off. The phenolic resin-derived carbon obtained by the described process has a S<sub>BET</sub> of 534 m<sup>2</sup>/g when non activated, for a particle size of 125-250 μm. This increases to 1057 m<sup>2</sup>/g at 30% activation; 1432 m<sup>2</sup>/g at 47% activation; 1703m<sup>2</sup>/g at 52% activation and 2018 m<sup>2</sup>/g at 65% activation. Phenolic carbons freshly activated in carbon dioxide had a point of zero charge of 10, indicating that at typical environmental water pH the surface of the carbon would be positively charged. Analysis of the surface chemistry of the carbon beads was carried out using Boehm titrations (Valente Nabais and Carrott, 2006). The range of phenolic carbons beads prepared did not have significant differences in their surface chemistry. Total carboxylic functions (mainly free carboxylic acid + anhydride + lactone + lactol) were 0.58 mmol/g as determined by back titration after reaction with Na<sub>2</sub>CO<sub>3</sub>. Total acidic functionalities were 1.16 mmol/g as determined by back titration after reaction with NaOH. Hence, the phenolic OH content was 0.58 mmol/g.

From the range of phenolic carbon prototypes synthesised, those with clear differences in their mesoporosity were tested for the adsorption of atrazine in a column flow through experiment (conditions and carbon prototype properties are given in Materials and methods). Phenolic carbons beads, named as TE3 and TE7 (prepared with 180 and 300 weight parts of ethylene glycol per 100 parts of the resin), had abundant microporosity, low and high meso- and macroporosity, and an S<sub>BET</sub> of 1057 and 1703 m<sup>2</sup>/g, respectively. The phenolic carbon beads with the highest active surface area and pore volume (TE7) gave the greatest uptake of

atrazine: 419 mg atrazine/g upon saturation. We previously showed that TE3 and TE7 effectively removed the emerging contaminant metaldehyde (Busquets et al., 2014).

To examine the effects of  $S_{\text{BET}}$  on the uptake of atrazine, TE7 carbons were synthesised with smaller particle size (40-60 $\mu\text{m}$ ), which had a 15% larger  $S_{\text{BET}}$ : 1942  $\text{m}^2/\text{g}$ . In this case, the maximum adsorptive capacity for atrazine increased to 641 mg atrazine/g carbon. This maximum adsorptive capacity would give a coverage of 1238  $\text{m}^2/\text{g}$  with atrazine according to the dimensions of the herbicide shown in in Figure 1. This represents 64% of the surface area of the carbon covered, and indicates that there are specific sites on the carbon where the pesticide adsorbs. This contrasts with the 18% surface coverage found for GAC. The TE7 carbons were found to be optimal: they have higher porosity and smaller particle size than GAC, both characteristics are considered important for the removal of atrazine and potentially for micropollutants of similar size. High adsorptive capacities (i.e. the phenolic carbon beads adsorbed atrazine to more than half their own weight) were found. **Figure 2** shows the structural properties of the carbons and their adsorption capacity under flow-through conditions. The pore size distribution diagrams (**Figure 2**, right) show that while the size of the micropores is similar in all the carbons, the size range of meso- and macropores increases from TE3 to TE7 mainly due to the larger amount of the pore former used.

### **Incorporation of phenolic carbon beads in a macroporous polymer matrix**

Although the prepared carbon beads were highly efficient for atrazine removal compared to conventional GAC, their relatively small particle size (particularly for the 40 - 60 $\mu\text{m}$  microbeads with higher active surface area) makes their use in conventional large scale water treatment problematic. In addition, use of small packed beads may significantly increase back pressures in column filtration mode. To overcome this, we examine here the effects of incorporating the beads into a macroporous polymer scaffold, specifically a PVA-derived cryogel or macroporous polymer structure (MPPS<sup>TM</sup> - see experimental). This scaffold allows

the preparation of elastic filters of various geometries and facilitates their repeated use for water filtration. The large macropores of the polymer gel matrix, approximately 100 to 200  $\mu\text{m}$  in diameter, allow flow through with low flow resistance, as well as keeping the active carbon surface accessible for adsorbing contaminants from water. Under the filtration conditions used, a 7% reduction of the flow rate was observed when using the composite. In contrast, no reduction was observed when the filtration was carried out through a microbead-packed column with the same dimensions as the composite. **Figure 3** shows a SEM image of the composite, and illustrates (i) the spherical carbon beads held by a thin PVA film (**Figure 3**, arrow A) and (ii) the macropores in the gel (**Figure 3**, arrow B). Hence, the filter is a hierarchical material; it contains carbon beads with a range of macro-, meso- and micropores that play an important role in contaminant removal within a macroporous scaffold.

The effect of coating part of the carbon surface with a polymer film on the adsorption kinetics was investigated by comparing the adsorption of atrazine on “free” carbon beads with that on the carbon-cryogel composite. The adsorbent and the atrazine solution were put in contact using two approaches: (a) manual shaking for 10 seconds, with samples then left to incubate at room temperature without further agitation; (b) under magnetic stirring. While the adsorption was faster in the free carbon beads in the absence of agitation, the adsorption capacity of the carbon beads embedded in PVA was not noticeably suppressed by the PVA film since the final concentration of atrazine in solution was approximately the same in both free carbon and carbon-filled PVA systems (**Figure 4a**). These static conditions were assayed to observe the maximum difference in diffusion between the “free” beads and the PVA-embedded beads. When the atrazine diffusion experiment was carried out under magnetic stirring, conditions which did not modify the structure of the particles, the adsorption was approximately twice as fast (**Figure 4b1**, **Figure 4b2**) compared to the non-agitated samples

(**Figure 4a1, Figure 4a2**). There was no significant adsorption of atrazine by PVA scaffolds without carbon beads (not shown) ( $P > 0.05$ ).

The fractional equilibrium ( $F$ ) was calculated at different adsorption times to allow the treatment of the kinetic data of **Figure 4** in dimensionless form. The figure in Supporting Information S7 shows  $F$  as a function of the square root of time (according to equation (4), Supporting information), for carbon beads (replicates: \*, o,  $\Delta$  in the figure) and for beads embedded in PVA cryogel (replicates:  $\square$ , +,  $\diamond$ ). The data indicate markedly faster uptake values for the carbon beads but with at least one order of magnitude lower pore diffusion coefficient ( $\bar{D}$  of  $4.2 \times 10^{-10} \text{ cm}^2/\text{s}$ ) compared to the diffusion when the beads were embedded in the cryogels ( $\bar{D}$  of  $2.5 \times 10^{-8} \text{ cm}^2/\text{s}$ ). This could be a consequence of the greater wettability of the PVA-carbon cryogels compared to the carbon microbeads and therefore, a higher accessibility of the adsorbent for atrazine in the aqueous solution.  $\bar{D}$  was calculated using a model proposed by Samsonov and Kuznetsova, 1992 (see equations 6 and 7 in Supporting information). The experiment performed under stirring conditions (which exhibited fast adsorption) had insufficient early data points to be analyzed by the first model (equation 4 in the Supporting Information). Only the data points that were taken after  $> 6$  min were used to fit a curve (equation 7 Supporting Information), and in that case  $\bar{D}$  was  $3.3 \times 10^{-9} \text{ cm}^2/\text{s}$ , i.e. higher than  $\bar{D}$  for the static carbon beads, which could be expected because magnetic stirring provides better mass transport and results in faster external diffusion of the solute to the carbon surface. Notably, the  $\bar{D}$  for the stirred carbon sample remained lower than the diffusion coefficient for the carbon-PVA under static conditions.

### **Mechanical properties**

The Young's modulus of elasticity of the composites studied was  $13.1 \pm 0.8 \text{ MPa}$  ( $n=8$ ), and the loading achieved at 75% compression was  $19.6 \pm 2.1 \text{ N}$  ( $n=8$ ), conditions that did not

break the monolith. **Figure 4S**, Supporting Information, displays the stress-strain curve of the composite, showing elastic behaviour under compression at moisture conditions representative of its state during filtration. Under the pressure exerted at  $39 \text{ h}^{-1}$  flow in the flow-through experiments (where the flow rate is expressed as liquid hourly space velocity), the carbon-cryogel composites were compressed by up to 23%. In contrast no compression was observed in a column packed with beads only.

#### **Flow-through experiments using carbon-cryogel composite filters.**

The purification performance of cryogel-carbon composites ( $\text{Ø}3 \times 85\text{mm}$  dimensions, containing 30 mg TE7 carbon beads) was tested at  $39 \text{ h}^{-1}$  (flow rate expressed as liquid hourly space velocity; liquid flow rate/bed volume) for the purification of atrazine ( $2\mu\text{g/L}$  spiked in ultrapure water and  $32\text{mg/L}$  spiked in: ultrapure water; ultrapure water containing 32 mg potassium hydrogen phthalate/L as a model of water with high organic carbon content; and estuarine water (Ouse river, Newhaven harbour, East Sussex, UK) the composition of which before spiking is described in Materials and methods). The  $39 \text{ h}^{-1}$  flow rate used was selected to exceed flows typically experienced in water treatment plants, to provide a more realistic flow-through scenario. Results are shown in **Figure 5** and **Table 1**.

Testing the developed filter materials with water containing a high content of organic matter, and also inorganic substances (i.e. high dissolved salts) in the case of estuarine water, mimics the effect of possible competing species at high concentration on atrazine removal. Tests with spiked water had TOC values an order of magnitude greater than typical surface water to determine filter performance under extreme conditions. **Figure 5** shows that a total water filtrate of  $>200$  bed volumes contained concentrations of atrazine  $<0.1\mu\text{g/L}$  compared to the inlet water containing  $32\text{mg/L}$  of atrazine. This was observed in the estuarine water sample and the water sample spiked at TOC levels an order of magnitude greater than typical surface water. The purification achieved when using concentrations of atrazine a million times

greater than some environmental levels reported (ca. 3 ng/L) (Loos et al., 2010), or in the same order of magnitude (Nogueira et al., 2012), illustrates the high capacity of the composite. For ultrapure water contaminated at 2 µg/L, 27400 bed volumes were filtered before the concentration of atrazine exceeded 0.1 µg/L. When these levels of atrazine were tested in batch mode, concentrations were below the limit of detection (see Supporting information S4) at equilibrium, hence the direct quantification of adsorption capacity was not possible at these concentrations.

Notably, the purification of a more complex matrix than ultrapure water, with high concentrations of soluble organic matter or high salinity, caused a relatively small drop in adsorption capacity, i.e. the amount of filtered water with safe levels of pesticide decreased by less than 30% (**Table 1**). This suggests that the sites adsorbing atrazine may have some size exclusion selectivity for the adsorption of small molecules such as atrazine, as the sites in the phenolic carbon retain their capacity to remove atrazine in the presence of high concentrations of potentially competing substances. This highlights their potential capacity for contaminant removal from other environmental, industrial or biological media. The slight decrease in adsorptive capacity observed when filtering estuarine water could be due to the blockage of transport pores under these high ionic strength conditions.

Removal of malathion, another polar pesticide with chemical structure different to atrazine, was also tested. In this case ultrapure water containing 16 mg malathion /L was filtered through the composite filter. The adsorptive capacity reached at the last safe filtrate fraction (0.1 µg/L) (Council of the European Communities, 1998) was 244 mg malathion/g carbon and 591 mg malathion/g carbon at the saturation of the carbon-cryogel composites, at 745 and 2533 bed volumes, respectively. Supporting information **Figure S8** shows the breakthrough curve for the purification of malathion. This result indicates that the high



purification capacity of the developed material is not specific to atrazine but also may apply to other polar pollutants

### **Cytotoxicity assays.**

Studies of the effect of carbon-cryogel filtered water on the viability of Caco-2 cells (**Figure 6**), which are the first type of cells that would be exposed to filtered water when drinking, indicated a significant reduction in cell viability associated with the first 10 mL aliquot filtered through the composite (P 0.05). No significant reduction in viability was observed however with subsequent aliquots (**Figure 6 A**) (P 0.05). While the MTS assay applied has been reliably used to assess cell viability and toxicity (Malich et al., 1997), the assay only assesses metabolic activities of mitochondria (Wang et al., 2010; McGowan et al., 2011). As such, the reduction in the conversion of MTS into formazan may not necessarily mean cell death. An LDH assay was therefore carried out to complement the MTS assay results. LDH is a cytoplasmic enzyme found in all cells and it can only be found extracellularly, such as in culture medium, in the event of cell membrane damage and/or cell death, where the amount of LDH released is proportional to the amount of dead cells (Jurisic, 2003; Smith et al., 2011). In this work, LDH assay results show no significant toxicity associated with water filtrate aliquots across all volumes, including the first 10 mL (**Figure 6 B**) (P 0.05). This suggests that the reduction in cell viability seen in the MTS assay is not due to cell death but rather to a compromised mitochondrial activity. Crucially however, this problem of reduced metabolic activity can be addressed by an initial pre-wash of the PVA-C membrane/column with a volume of water that is 5 times the bed volume prior to use. Previous work has indicated that the carbon beads used in the composite filter do not produce a cytotoxic response against a V79 cell line (Barnes et al, 2009).

**Potential implementation for water clean-up.** The developed composites have shown high purification capacity at lab scale at liquid hourly space velocities ( $39\text{h}^{-1}$ ) which are greater

than typical flow rates applied in water treatment plants. This makes them potentially useful both for low flow rate applications and for larger scale applications with higher flow rates and larger water volumes. Recent work by the authors (Savina et al., 2016) shows that cryogel-based composites of the type described here can be produced in volumes of 400mL or greater in a monolithic (i.e. column filter) form with uniform pore size and carbon particle distribution, indicating the potential scalability of the filters. The use of a flexible polymer scaffold produced via cryogelation also means that the composite filters can be produced in a variety of shapes: sheets for reactive barriers, discs, beads or monoliths (Savina et al., 2011), or within robust plastic carriers (Le Noir et al., 2009; Plieva et al., 2006) for more aggressive physical settings (e.g. in settlement tanks, fluidised beds, etc.). This provides significant flexibility in terms of device configuration.

#### **4. Conclusions**

Effective filters with superior adsorptive capacity for the removal of polar micropollutants, based on PVA macroporous cryogels with embedded phenolic carbon microbeads with controllable porosity, have been developed and tested for the treatment of contaminated water with high TOC levels. Embedding the carbon beads in a polymer support retains the adsorptive capacity of the carbons while improving the pore diffusion. The structure of the phenolic carbons, their micro- and mesopores, high  $S_{\text{BET}}$  and small particle size were shown to play an important role in the high adsorptive capacity of the filter. Adsorptive capacities of up to 641 mg atrazine/g carbon and 591 mg malathion/g carbon were obtained when filtering water containing 32 mg atrazine/L and 16 mg malathion/L (and 1.4% ethanol) in flow through experiments at  $39 \text{ h}^{-1}$ . The cytotoxicity of water passed through the filter at the same flow rate was tested with human epithelial cells, and no toxicity was found from 17-1667 bed

volumes. Prototypes developed at the lab scale are a promising water purification technology with superior adsorptive capacity.

## **Acknowledgements**

We thank the Industry-Academia Partnership and Pathways Scheme (Carbosorb, project no. 230676) and Intra European Fellowship Scheme (Polarclean, project N<sup>o</sup>. 274985), from the EC Seventh Framework Programme Marie Curie Actions, for financial support. Dr Howard Dodd, Chris English, Peter Lyons, Sandeep Kumar, Yishan Zheng and Petra Kristova (all University of Brighton) are acknowledged for their technical support. The contribution from anonymous reviewers is acknowledged.

## **REFERENCES**

Barnes, L.M., Phillips, G. J. J., Davies, G., Lloyd, A. W., Cheek, E., Tennison, S.R., Rawlinson, A. P., Kozynchenko, O. P., Mikhalovsky, S.V., 2009. The cytotoxicity of highly porous medical carbon adsorbents. *Carbon* 47, 1887–1895.

Busquets, R., Kozynchenko, O. P., Whitby, R. L.D., Tennison, S.R., Cundy, A. B., 2014. Phenolic carbon tailored for the removal of polar organic contaminants from water: A solution to the metaldehyde problem?. *Water Res.* 15, 46-56.

Cabezam, Y., Candela, L., Ronen, D., Teijon, G., 2012. Monitoring the occurrence of emerging contaminants in treated wastewater and groundwater between 2008 and 2010. The Baix Llobregat (Barcelona, Spain). *J. Hazard. Mater.* 32, 239-240.

Council of the European Communities, 1998. Directive of the European Parliament and of the Council on the quality of water intended for human consumption. (98/83/EC).

Fadaei, A., Dehghani, M. H., Nasser, S., Mahvi, A. H., Rastkari, N., Shayeghi, M., 2012. Organophosphorous pesticides in surface water of Iran. *B. Environ. Contam. Tox.* 88, 867-869.

Fent, K., Weston, A., Caminada, D., 2006. Ecotoxicology of human pharmaceuticals. *Aquat. Toxicol.* 76, 122-159.

Gueudré, L., Milina, M., Mitchell, S., Pérez-Ramírez, J., 2014. Superior mass transfer properties of technical zeolite bodies with hierarchical porosity. *Adv. Funct. Mater.* 24, 209-219.

Homem, V., Silva, J.A., Ratola, N., Santo, L., Alves, A., 2015. Long lasting perfume; A review of synthetic musks in WWTPs. *J. Environ. Manage.* 149, 168-192

Ifelebuegu, A. O., 2011. The fate and behaviour of selected endocrine disrupting chemicals in full scale wastewater and sludge treatment unit processes. *Int. J. Environ. Sci. Tech.* 8, 245-254.

Jeong, C. H., Wagner, E. D., Siebert, V. R., Anduri, S., Richardson, S. D., Daiber, E. J., McKague, A. B., Kogevinas, M., Villanueva, C. M., Goslan, E. H., Luo, W., Isabelle, L. M., Pankow, J. F., Grazuleviciene, R., Cordier, S., Edwards, S. C., Righi, E., Nieuwenhuijsen, M. J., Plewa, M. J., 2012. Occurrence and toxicity of disinfection byproducts in European

drinking waters in relation with the HIWATE epidemiology study. *Environ. Sci. Technol.* 46, 12120-12128.

Ji, L., Liu, F., Xu, Z., Zheng, S., Zhu, D., 2010. Adsorption of pharmaceutical antibiotics on template-synthesized ordered micro- and mesoporous carbons. *Environ. Sci. Technol.* 44, 3116-3122.

Juriscic, V., 2003. Estimation of cell membrane alteration after drug treatment by LDH release. *Blood* 101, 2894.

Kokotou, M. G., Asimakopoulos, A. G., Thomaidis, N. S., 2012. Artificial sweeteners as emerging pollutants in the environment: analytical methodologies and environmental impact. *Anal. Methods* 4, 3057-3070.

Le Noir, M., Plieva, F. M., Mattiasson, B., 2009. Removal of endocrine-disrupting compounds from water using macroporous molecularly imprinted cryogels in a moving-bed reactor. *J. Sep. Sci.* 32, 1471-1479.

Loos, R., Locoro, G., Contini, S., 2010. Occurrence of polar organic contaminants in the dissolved water phase of the Danube River and its major tributaries using SPE-LC-MS<sup>2</sup> analysis. *Water Res.* 44, 2325-2335.

Loos, R., Carvalho, R., Antonio, D.C, Comero, S., Locoro, G., Tavazzi, S., Paracchini, B., Ghiani, M., Lettieri, T., Blaha L., Jarosova, B., Voorspoels, S., Servaes K.,

Haglund, P., Fick, J., Lindberg, R.H., Schwesig, D., Gawlik, B. M., 2013. EU-wide monitoring survey on emerging polar organic contaminants in wastewater treatment plant effluents. *Water Res.* 47, 6475-6487.

Malich, G., Markovic, B., Winder, C., 1997. The sensitivity and specificity of the MTS tetrazolium assay for detecting the in vitro cytotoxicity of 20 chemicals using human cell lines. *Toxicology* 124, 179-192.

McGowan, E. M., Alling, N., Jackson, E. A., Yagoub, D., Haass, N. K., Allen, J. D., Martinello-Wilks, R., 2011. Evaluation of cell cycle arrest in estrogen responsive MCF-7 breast cancer cells: pitfalls of the MTS assay. *PLoS ONE*, 6, e20623, 1-8.

Nogueira, E. N., Dores, E. F. G. C., Pinto, A. A., Amorim, R. S. S., Ribeiro, M. L., Lourencetti, C., 2012. Currently used pesticides in water matrices in Central-Western Brazil. *J. Braz. Chem. Soc.* 23, 1476-1487.

Plieva, F. M., Karlsson, M., Aguilar, M.R., Gomez, D., Mikhalovsky, S., Galaev, I.Y., Mattiason, B., 2006. Pore structure of macroporous monolithic cryogels prepared from poly(vinyl alcohol). *J. Appl. Polym. Sci.* 100, 1057-1066.

Richardson, S. D. T., Ternes A., 2014. Water analysis: emerging contaminations and current issues. *Anal. Chem.* 86, 2813-2848.

Samsonov, G.V., Kuznetsova, N. P., 1992. Crosslinked polyelectrolytes in biology, in: Abe.A., Dus̃ek, K., Kobayashi, S. (Eds.), *Polyelectrolytes hydrogels chromatographic*

materials, *Advances in Polymer Science*. Springer-Verlag, Berlin, Germany, pp 1-50,. ISBN: 3-540-55109-3; 0-387-55109-3.

Savina, I.N., English, C. J., Whitby, R. L.D., Zheng, Y., Leistner, A., Mikhalovsky, S. V., Cundy, A. B., 2011. High efficiency removal of dissolved As(III) using iron nanoparticle-embedded macroporous polymer composites. *J. Hazard. Mater.* 192, 1002-1008.

Savina, I.N., Ingavle, G.C., Cundy, A.B., Mikhalovsky, S.V., 2016. A simple method for the production of large volume 3D macroporous hydrogels for advanced biotechnological, medical and environmental applications. *Scientific Reports*, 6:21154, 1-9

Sorensen, J.P.R., Lapworth, D.J., Nkhuwa, D.C.W., Stuart M.E., Gooddy, D.C., Bell, R.A., Chirwa, M., Kabika, J., Liemisa, M., Chibesa, M., Pedley, S., 2015. Emerging contaminants in urban groundwater sources in Africa. *Water Res.* 72, 51-63.

Smith, S. M., Wunder, M. B., Norris, D. A., Shellman, Y. G., 2011. A simple protocol for using a LDH-based cytotoxicity assay to assess the effects of death and growth inhibition at the same time. *PLoS ONE*, 6, e26908.

Tenninson, S. R., Kozynchenko, O. P., Volodymyr, V. S.; Blackburn, J., 2000. Porous Carbons, WO2001GB03560 20010807, US2011097583.

Unur E., 2013. Functional nanoporous carbons from hydrothermally treated biomass for environmental purification. *Micropor. Mesopor. Mat.* 168, 92-101.

US EPA, Decision documents for atrazine, Washington DC, USA, 2006.  
[http://www.epa.gov/oppsrrd1/REDS/atrazine\\_combined\\_docs.pdf](http://www.epa.gov/oppsrrd1/REDS/atrazine_combined_docs.pdf).

Valente Nabais, J. M., Carrott, P. J. M., 2006. Chemical characterization of activated carbon fibers and activated carbons. *Journal Chem. Educ.* 83, 436-438.

Varca, L. M., 2012. Pesticide residues in surface waters of Pagsanjan-Lumban catchment of Laguna de Bay, Philippines. *Agr. Water Manage.* 106, 35-41.

Wang, P., Henning, S. M., Heber, D., 2010. Limitations of MTT and MTS-based assays for measurement of antiproliferative activity of green tea polyphenols. *PLoS ONE*, 5, e10202.

Wilkinson, J.L., Swinden, J., Hooda, P., Barker, J., Barton, S., 2016. Markers of anthropogenic contamination: A validated method for quantification of pharmaceuticals, illicit drug metabolites, perfluorinated compounds, and plasticisers in sewage treatment effluent and rain runoff. *Chemosphere* 159, 638–646.

WHO (World Health Organisation), 2004. Malathion in drinking-water. Background document for development of WHO guidelines for drinking-water quality. Available from [http://www.who.int/water\\_sanitation\\_health/dwq/chemicals/malathion.pdf](http://www.who.int/water_sanitation_health/dwq/chemicals/malathion.pdf) (accessed May 2014).



Zhang, Y., Xu, S., Luo, Y., Pan, S., Ding, H., Li G., 2011. Synthesis of mesoporous carbon capsules encapsulated with magnetite nanoparticles and their application in wastewater treatment. *J. Mater. Chem.* 21, 3664-3671.

### Figure Captions

**Figure 1.** Diagram showing the dimensions of an optimal carbon structure for adsorption of atrazine.

**Figure 2.** Breakthrough curves for the adsorption of atrazine on different phenolic carbons packed in a column with dimensions 5x70mm. TE7 40-60 $\mu$ m particle size (73 mg of carbon) (■); TE7 125-250 $\mu$ m particle size (195 mg of carbon) (●); TE3 125-250  $\mu$ m particle size (352 mg carbon) (▲). The adsorption capacities at the last safe water filtrate fraction (below 0.1  $\mu$ g/L) and saturation point of the curves are given. The pore size distribution of the carbons is also shown.

**Figure 3.** SEM image of the water purification device based on carbon microbeads embedded in a macroporous PVA cryogel.

**Figure 4.** Uptake of atrazine by carbon beads (a1, b1), replicates shown as \*, o,  $\Delta$ , and beads embedded in cryogel (a2, b2), replicates shown as  $\square$ , +,  $\diamond$ , under static (a1, a2) and dynamic (magnetically stirred) conditions (b1, b2).

**Figure 5.** Removal of atrazine spiked at 32 mg/L in ultrapure water with 1.4% ethanol (■); ultrapure water with potassium hydrogen phthalate added at the same concentration as atrazine (32 mg/L) (●); estuarine water (▲) by a carbon-cryogel composite (1.5 i.d x 85 mm, 0.6 ml bed volume). A chromatogram of atrazine and full scan mass spectra of atrazine  $m/z$   $[M+H]^+$  216 and D<sub>5</sub>-atrazine  $m/z$   $[M+H]^+$  221 are shown.

**Figure 6** Viability of Caco-2 cells exposed to (ultrapure) water passed through a PVA-C column. (A) Cell viability as determined by MTS assay and (B) cytotoxicity as determined by LDH assay. In the MTS assay, control (+) corresponds to cells that did not receive treatment with PVA-C filtrate water. In the LDH assay, control (+) and (-) represent total cell death and cells that did not receive PVA-C filtrate water, respectively.

Journal of Environmental Management.

Supplementary material

**Carbon-Cryogel Hierarchical Composites as Effective and Scalable Filters for Removal of Trace Organic Pollutants from Water**

Rosa Busquets<sup>1,3,7\*</sup>; Alexander. E. Ivanov<sup>2</sup>; Lubinda Mbundi<sup>1,5</sup>, Sofia Hörberg<sup>2</sup>, Oleksandr P. Kozynchenko<sup>3</sup>; Peter J. Cragg<sup>1</sup>; Irina N. Savina<sup>1</sup>; Raymond L.D. Whitby<sup>1,4</sup>; Sergey V. Mikhalovsky<sup>1,4</sup>; Stephen R. Tennison<sup>3</sup>; Hans Jungvid<sup>2</sup>; Andrew B.Cundy<sup>1,6\*</sup>.

<sup>1</sup>University of Brighton, Faculty of Science and Engineering, BN2 4GJ, UK

<sup>2</sup>Protista Biotechnology AB, Kvarngatan 2, P.O. Box 86 SE- 267 22 Bjuv, Sweden

<sup>3</sup>MAST Carbon International Ltd. Jays Close, Basingstoke, Hampshire RG22 4BA, UK†

<sup>4</sup>Nazarbayev University, School of Engineering, 53, Kabanbay Batyr Ave., Astana, 010000, Kazakhstan

<sup>5</sup>Blond McIndoe Research Foundation, East Grinstead, RH19 3DZ, UK

<sup>6</sup>University of Southampton, School of Ocean and Earth Science, Southampton, SO14 3ZH, UK.

<sup>7</sup>Kingston University, Faculty of Science, Engineering and Computing, Kingston Upon Thames, KT1 2EE, UK

### **Author information**

\* e-mail: A.Cundy@soton.ac.uk

\* e-mail: R.Busquets@Kingston.ac.uk

9 PAGES

TABLE OF CONTENTS

**S1.** Text describing the source/purity of chemicals.

**S2.** Materials and methods used in the structural characterisation of the filter.

**S3.** Formula for the quantification of adsorption capacity and equations for the calculations of pore diffusion kinetics, fractional equilibrium, and diffusion coefficient

**S4** Stress-strain curve obtained for the composite

**S5.** Methodology for the quantification TC, IC, TOC and major cations in the estuarine water and atrazine and malathion in the purified water fractions.

**S6.** Cell culture materials and methods

**S7** The fractional equilibrium versus the square root of time.

**S8.** A breakthrough curve showing the removal of malathion from water with the composite.

**S1.** Poly(vinyl alcohol) (PVA), Mowiol 18-88 with  $M_w = 130000 \text{ g}\cdot\text{mol}^{-1}$  and saponification degree of 88%, was used in the synthesis of the polymer scaffold and was purchased from Clariant GmbH (Frankfurt, Germany). Aqueous glutaraldehyde (GA) solution (50%, photographic grade) was from Sigma-Aldrich, Stenheim, Germany. Sodium cyanoborohydride (>95%) was a product of Merck Schuchardt OHG (Hohenbrunn, Germany). Atrazine and 2-chloro-4-ethyl-d<sub>5</sub>-amino-6-isopropylamino-1,3,5-triazine (D<sub>5</sub>-atrazine) (99% purity) and malathion (97% purity) were Pestanal<sup>®</sup> Fluka standards purchased at Sigma Aldrich (UK). Ultrapure water (TOC 8  $\mu\text{g}$  carbon/L, resistivity 15 Megohm·cm, pH 7.9) was obtained with an ELGA Purelab purification system (Veolia, UK). The kits CellTiter 96<sup>®</sup> Aqueous Non-Radioactive Cell Proliferation Assay (MTS) and CellTox<sup>™</sup> Green Cytotoxicity Assay (LDH) were purchased from Promega (UK). Cell Media DMEM/HAM F12 without L-glutamine and stable glutamine-ATMP-ready were purchased at PAA laboratories Ltd.

**S2.** Table S2. Structural properties of GAC, and a meso- (TE3) and meso-macroporous phenolic carbon (TE7)

Type of carbon beads (particle size)	SBET ( $\text{m}^2/\text{g}$ )	$V_{0.99}$ ( $\text{cm}^3/\text{g}$ )	Dominant porosity according to nitrogen isotherms
GAC (3mm)	552	1.04	microporosity
TE3 (125-250 $\mu\text{m}$ )	1057	1.14	mesoporosity
TE7 (125-250 $\mu\text{m}$ )	1703	1.65	meso-macroporosity
TE7 embedded in cryogel scaffold (40-60 $\mu\text{m}$ )	1939	1.82	meso-macroporosity

**S2.** Nitrogen adsorption-desorption isotherms. Beads were previously degassed for 24h at 130 °C. The specific surface area ( $S_{\text{BET}}$ ) was calculated according to the standard BET method (Gregg, Sing, 1995). The total pore volume,  $V_p$ , was evaluated at  $P/P_0$  0.99, where P and  $P_0$

denote equilibrium pressure and the saturation pressure of nitrogen at 77.4 K, respectively.

Pore size distributions were analysed using the BJH method and non-local density functional theory (Gregg, Sing, 1995). The carbon: cryogel composites were freeze dried, sputter coated with palladium and examined using a JEOL JSM-6310 (Oxford Instruments) scanning electron microscope.

**S3.** Formula for the quantification of adsorption capacity and equations for the calculations of pore diffusion kinetics, fractional equilibrium, and diffusion coefficient

The quantification of the adsorptive capacity for atrazine and pore diffusion kinetics.

The adsorbed amount of atrazine was calculated for each sample using the formula:

$$m_{\text{atrazine}} = (C_0 - C_\infty) \cdot V \cdot M_{\text{atrazine}} \quad (2)$$

where  $m_{\text{atrazine}}$  is the adsorbed amount of atrazine in mg,  $C_0$  and  $C_\infty$  are the initial and equilibrium concentrations of atrazine in  $M$  in the aqueous solution in contact with the adsorbent.  $V$  is the volume of the atrazine solution in ml and  $M_{\text{atrazine}}$  is the molar mass of atrazine ( $M_{\text{atrazine}} = 215.68$  g/mol). The weight of the adsorbed atrazine was divided by the weight of the carbon powder in the samples.

The fractional equilibrium  $F$  was calculated from the data points in the kinetic curves using

$$\text{the equation: } F = \frac{C_0 - C_t}{C_0 - C_\infty}$$

(3)

Where  $C_0$  and  $C_\infty$  are the initial and equilibrium concentration of pesticide in the aqueous solution.  $C_t$  is the instantaneous concentration of pesticide. The first model used to calculate  $\bar{D}$  describes the initial part of the curve to obtain the diffusion coefficient. In the equations 3-8,  $R$  corresponds to the diameter of the particle (carbon bead or cryogel-carbon) being tested.

$$F \approx \frac{6}{R} \sqrt{\frac{\bar{D}t}{\pi}} - 3 \frac{\bar{D}t}{R^2} \quad (4)$$

This model is mostly valid for relatively short incubation times

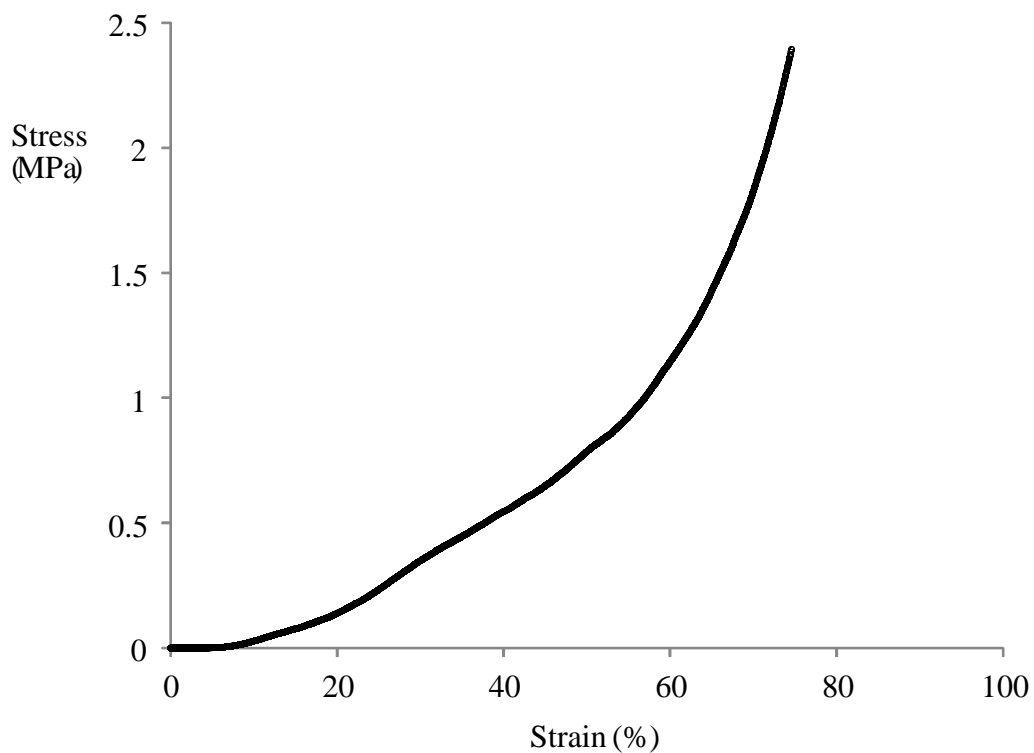
$$t < 0.15R^2/\bar{D} \quad (5)$$

For long incubation times, a second model was fitted to  $F = 1 - \frac{6}{\pi^2} e^{-\frac{\pi^2 \bar{D} t}{R^2}}$  (6)

The model can be linearized as follows:  $\ln(1 - F) = \ln\left(\frac{6}{\pi^2}\right) - \frac{\pi^2 \bar{D} t}{R^2}$  (7)

This model (6) is valid for relatively long incubation times:  $\frac{\bar{D} t}{R^2} > 0.15$ . (8)

#### S4. Stress-strain curve for the PVA-carbon composite



S5. Estuarine water from the Ouse river at Newhaven harbour, Sussex, UK, was analysed for total carbon (TC) and total inorganic carbon (IC) with a Shimadzu TOC-V CSH/CSN analyser (Kyoto, Japan), filtered through glass wool and used for adsorption studies within

24h of collection. Hydrochloric acid (2M) was used for the determination of IC. Total organic carbon (TOC) was determined by the difference between TC and IC. For the TC and IC analysis, glassware was rinsed with ultrapure water and acetone and dried before used. The analyses were carried out in triplicate and blanks were run in between samples. Major cations were analysed using a Perkin Elmer Optima™ 2100DV ICP-OES system after dilution with ultrapure water. The pH of the estuarine water was 8.1.

An LC system from Agilent Technologies (USA) model Series 1100 coupled to an ion trap mass spectrometer model Esquire (Bruker Daltonik GmbH) equipped with an off-axis electrospray working in positive mode was used for the determination of the pesticides. Data acquisition was carried out with Compass 2.0 software. The separation was carried out by fast chromatography using an Ascentis express fused core C<sub>18</sub> column with 2.7 µm particle size, 100 mm × 2.1mm I.D (Sigma-Aldrich GmbH) at a flow rate of 0.25 ml/min in isocratic conditions; 67% methanol in water at 40 °C. Standard mixtures containing atrazine and malathion, at concentration ranging from 8 µg/L to 0.7 mg/L, and D<sub>5</sub>-atrazine as internal standard at a concentration of 0.1 mg/L were prepared by weight for the calibration curves from the dilution of their respective stock standard solutions (1000 mg/L) prepared in methanol.

The injection volume was 5 µl for concentrations above 5 µg/L, and was increased to 25 µl for the analysis of lower concentrations, achieving a limit of detection (LOD) with a signal-to-noise ratio of 3 of 0.05µg atrazine/L and 0.1 µg malathion/L. The determination of atrazine was carried out in full scan mode (scan range  $m/z$  200-230), using the ions  $m/z$  216 [M+H]<sup>+</sup>, for atrazine and  $m/z$  221[M+H]<sup>+</sup> for D<sub>5</sub>-atrazine. The quantification of atrazine was carried out via isotopic dilution. The determination of malathion was carried out in product ion scan mode with  $m/z$  331 [M+H]<sup>+</sup> as precursor ion and  $m/z$  285 [M-(C<sub>2</sub>H<sub>5</sub>O)]<sup>+</sup> as product ion for the quantification (scan range  $m/z$  100-350). The product ion  $m/z$  210 [D<sub>5</sub>-atrazine -CH<sub>3</sub>]<sup>+</sup>

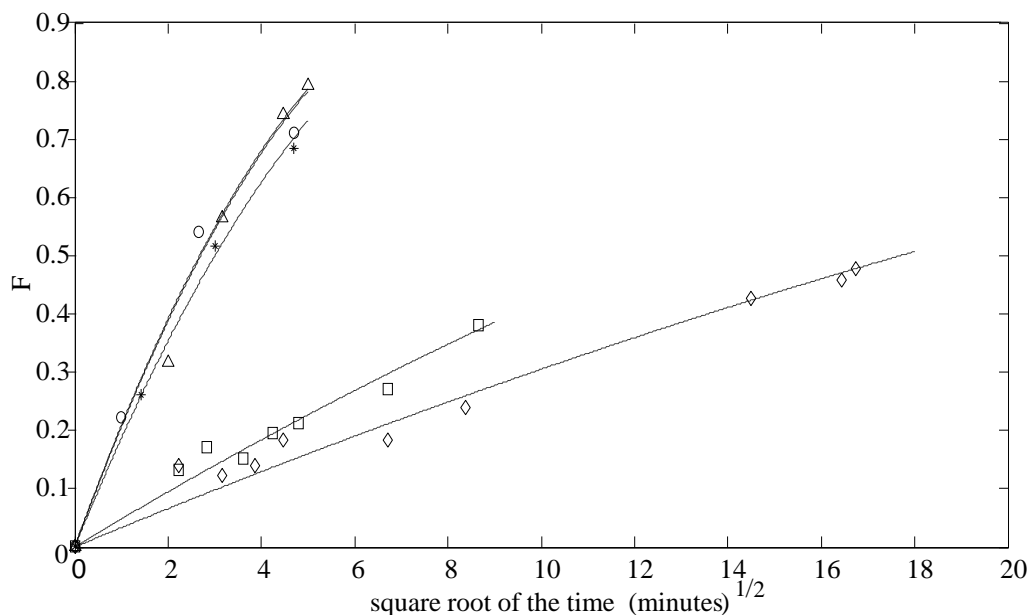


was used as the internal standard in the analysis of malathion. Both fragmentations were carried out at a fragmentation amplitude of 1.0 V. The determination of malathion in water was carried out by external calibration. In the analysis of atrazine and malathion, short term precision (n=6) assessed at 25 µg/L was 5% for atrazine and 6% for malathion. The optimal conditions of the electrospray were nebuliser gas (N<sub>2</sub>) 55.0 psi, dry gas (N<sub>2</sub>) 12 L/min and 360 °C as dry temperature. The optimal potential applied in the ion optics were capillary -4500V; end plate offset -500V; skimmer 38.7V; capillary exit 115.6V; octapole 1 DC 8.91V; octapole 2 DC 1.43V; octapole RF 160.7 V; lens 1, -10.9V; and lens 2, -67.5V.

**S6. Cytotoxicity study.** Heterogeneous human epithelial colorectal adenocarcinoma cells (Caco-2) were cultured in DMEM/Ham's F12 culture medium (supplemented with 10 % foetal bovine serum, 2.5 mM L-glutamine, and 100 IU/ml penicillin-streptomycin) from PAA, UK, to 85 % confluence (5 days) with media replacement every 3 days. The cells were transferred into 96 cell well plates at a seeding density of 2000 cells/well in culture medium which contained freeze-dried and reconstituted carbon-cryogel filtered water and incubated (37 °C, 5% CO<sub>2</sub>, 95 % humidity) for 24 hours. Briefly, ultrapure water was filtered through PVA-C cryogel (0.6 ml bed volume) and 10 ml aliquots were collected at different intervals (0-10, 11-20, 21-30, 31-40, 41-50, 491-500, 691-700, 841-850 and 991-1000 ml), freeze-dried in 20 ml polypropylene centrifuge tubes and reconstituted with 10 ml culture medium. Cells were then incubated in this culture medium. The water filtration and lyophilisation was carried out under non sterile conditions. The test tubes containing the lyophilised residue from the water filtrate were UV-sterilised for 1h before the reconstitution with culture media. After incubating for 24 hours, the culture medium was centrifuged to remove debris and cytotoxicity was assessed using the *In Vitro* Toxicology Assay Kit, lactic dehydrogenase (LDH) based TOX7 (Sigma Aldrich, UK) according to manufacturer instructions. The amount of LDH in the culture medium was determined spectrophotometrically at an

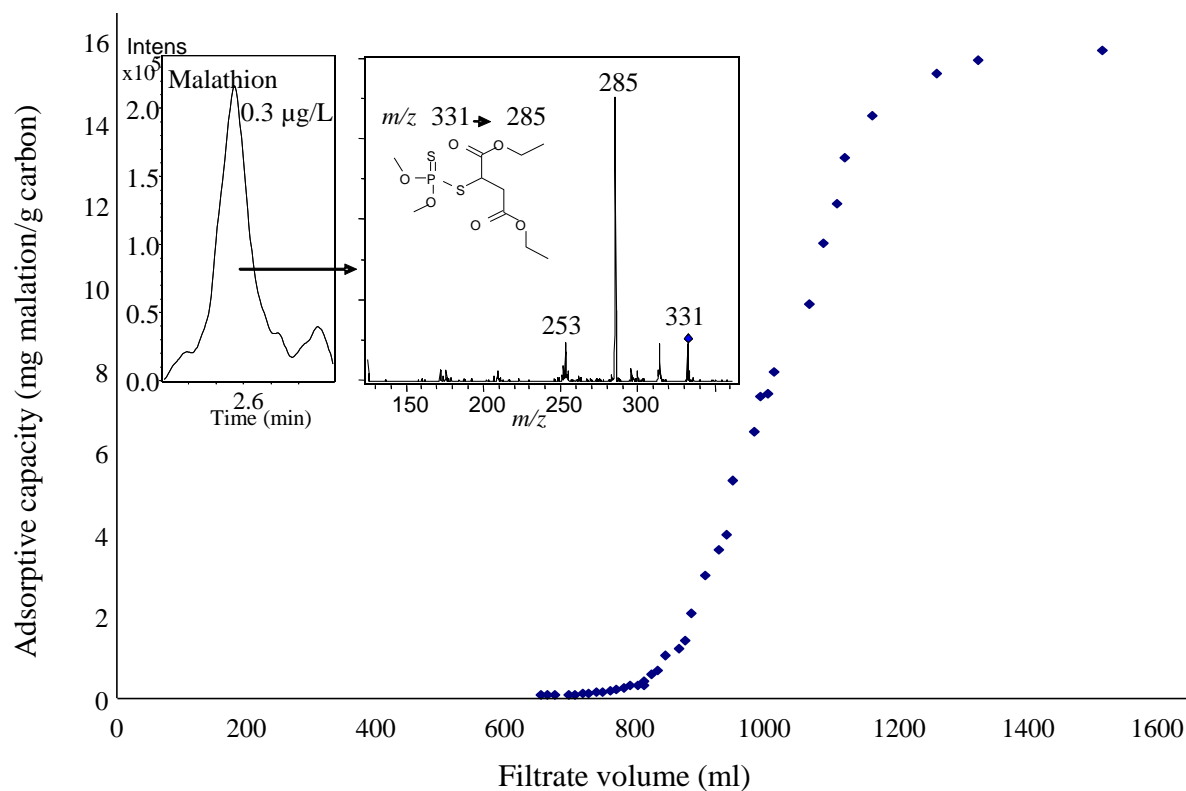
absorbance wavelength of 490 nm. The cells used as positive control for LDH assay were deliberately lysed for total LDH release and cells not treated with the water filtrate were used as a negative control. Cell viability was then assessed by analysing the ability of the cells to reduce MTS to formazan using CellTiter 96<sup>®</sup> Aqueous Non-Radioactive Cell Proliferation Assay Kit (Promega, UK). The amount of formazan in culture was determined spectrophotometrically at an absorbance wavelength of 490 nm. The MTS control cells were not treated with the water filtrate.

**S7** The fractional equilibrium versus the square root of time. The dotted lines are curves fitted to the different data points. Replicate experiments with carbon beads ( \*;o,Δ) and carbon-PVA (□, ◇) are shown.



**S8.** Breakthrough curve showing the removal of malathion spiked at 15.7 mg/L in ultrapure water by cryogel-carbon composite (1.5 i.d x 85 mm, 0.6 ml bed volume). The chromatogram

of malathion and its MS/MS spectra in one of the first filtered fractions is given. The flow rate used was  $39 \text{ h}^{-1}$ .



## REFERENCE

Gregg, S.J., Sing, K.S.W., 1995. Adsorption, surface area, and porosity, second edition, reprinted. Academic Press, London, UK.